

## Harnessing Electric Fields for Microfluidics – From Lightning Sparks to Tiny Tornadoes

Leslie Y. Yeo<sup>1</sup> and James R. Friend<sup>1</sup>

<sup>1</sup>Micro/Nanophysics Research Laboratory  
Monash University, Clayton, VIC 3800, AUSTRALIA

### Abstract

The dominance of surface tension and viscous effects over body forces such as inertia, gravity or centrifugal force makes fluid actuation and particle manipulation at microscale dimensions extremely difficult. We demonstrate the possibility of exploiting electric fields to drive unstable turbulent-like flows for micro-mixing and complex flows for efficient particle separation and concentration. In particular, the ions resulting from the breakdown of air surrounding a theoretically singular sharp electrode tip due to corona discharge is employed to accelerate the air towards the surface of a liquid in a cylindrical microchamber. Through interfacial shear, the surface liquid layer is recirculated to produce a Batchelor-type flow within the chamber that spirals suspended colloidal particles to a stagnation point at the bottom no-slip plane. We show the use of this technology for rapid and efficient separation of red blood cells from plasma for the development of miniaturised point-of-care diagnostics. Such liquid flows also become unstable at high applied voltages and frequencies leading to the generation of vortices that span a cascade of length scales, which can be exploited for micro-mixing.

### Introduction

Microfluidics is concerned with the actuation and manipulation of liquids and particles at microscale dimensions [6]. Since the characteristic length scales of typical biological systems are micron or sub-micron order, and since biomolecules are commonly transported within carrier fluids both *in vitro* and *in vivo*, microfluidics has played a huge role in advances associated with biotechnology and biomedical engineering. The many benefits of miniaturisation (e.g., enhanced transport, low costs, automation and parallelisation, etc.) has also resulted in significant interest in using microfluidics for chemical analysis, environmental diagnostics and portable fuel cells.

Nevertheless, there are substantial challenges for microscale liquid actuation and particle manipulation, not least the dominance of certain physical phenomena that would otherwise be less significant in comparison to other phenomena in macroscopic systems. One example is the surface area to volume ratio, which scales as the inverse of the characteristic length scale of the system. At microscopic dimensions, therefore, surface and viscous forces become important compared to body forces such as inertia, gravity and centrifugal forces. Such considerations thus needs to be accounted for in the design of efficient microfluidic systems.

For example, rotation and centrifugation, which are commonly employed for mixing and separations, cannot be easily generated in microsystems, at least without mechanically moving parts which are susceptible to reliability concerns at these small scales. Turbulence is also difficult to generate due to viscous effects overwhelming inertial forces; the Reynolds numbers in typical microfluidic systems are often below 0.1. Even in common electrokinetic devices, the proportionality between the velocity and electric fields in classical electroosmotic flows with constant  $\zeta$ -potential suggests that mixing vortices are virtually

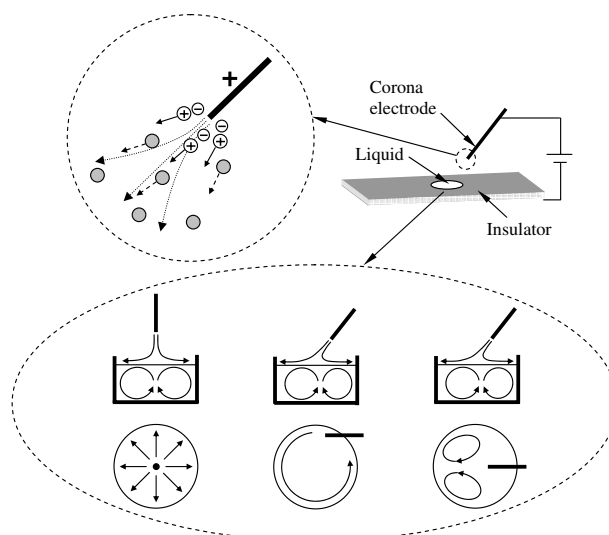


Figure 1: Generation of liquid recirculation in a microchamber 8 mm wide and 4 mm deep through interfacial air shear. The air flow arises due to the ionic wind mechanism depicted in the top left figure inset when the sharp electrode tip is raised to a voltage beyond the threshold ionisation potential. Depending on the orientation of the sharp electrode, various liquid recirculation patterns are observed, as shown by the illustrations in the bottom inset. The bulk liquid recirculation is a secondary phenomenon accompanying the primary surface recirculation.

impossible to generate due to the irrotationality of the electric field. In this article, we briefly discuss a novel and interesting phenomena that arises when gas phase electric fields are employed to drive liquid recirculation in a cylindrical microchamber for various microfluidic applications in which mixing, separation or particle trapping/concentration is required.

### Small Lightning Sparks, Mini Breezes and Tiny Tornadoes

Corona discharge occurs when the electric field in a gas phase exceeds a certain threshold such that there is electrical breakdown, giving rise to gas phase ions known as plasma. For instance, corona discharge occurs around the near-singular field around a sharp pointed electrode, such as a needle. As depicted in figure 1, co-ions are then accelerated away from the electrode due to repulsion, colliding into other electroneutral air molecules in its path. The momentum transfer that ensues then gives rise to an air flow known as *ionic wind*. It is then possible to generate the surface recirculation patterns as shown in the bottom inset of figure 1 by orientating the needle such that the air flow shears the liquid surface [9]. Further details of the experimental setup of the device is given elsewhere [1, 8, 9].

The surface recirculation is also accompanied by a corresponding recirculation in the bulk of the liquid beneath, as illustrated in the inset at the bottom of figure 1 [8]. Given the ionic wind driven surface recirculation at the top and the stationary base at

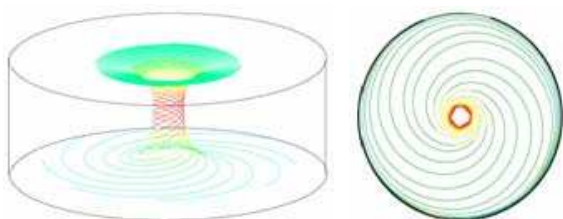


Figure 2: Spiral-like liquid trajectory of the secondary bulk motion arising due to the primary azimuthal rotation at the top surface and constrained by the stationary base, obtained from a numerical simulation of the governing hydrodynamic equations within the confines of the microchamber. The left image shows a three-dimensional construction of the flow field whereas the right image shows the flow cross-section in the Ekman boundary layer.

the bottom of the microchamber, the bulk recirculation is reminiscent of Batchelor flows that arise between liquid trapped between a stationary and rotating disk [2]. The flow trajectory is shown in figure 2, in which it is observed that the liquid spirals towards a central point at the base due to the suppression of centrifugal forces in the thin boundary layer adjacent to the stationary base known as the Ekman layer as a result of the no-slip condition at the bottom stationary surface. Flow conservation then requires the fluid to recirculate back up a central spinal column.

### Primary Surface Recirculation

Both surface and bulk recirculatory flows can be exploited for various microfluidic applications. Figure 3 shows colloidal microparticles which are attracted into and trapped within the surface vortices. It is mostly likely that the attraction mechanism arises from positive dielectrophoresis [5]. Once sufficient number of particles enter the vortex streamlines such that the limit of close packing is reached, shear induced diffusion [4] occurs whereby the particles begin to migrate from the external vortex streamlines where the shear is highest into the interior vortex streamlines where the shear is low [9]. This constitutes a simple but yet rapid mechanism for trapping and concentrating particles, particularly for enhancing online detection in miniature biosensor devices. This rapid particle concentration mechanism can also be exploited to enhance the collective fluorescent signal in bead-based diagnostics which employ fluorescent tagging of nanocolloids for specific antibody-antigen, protein-DNA or DNA-DNA complex assays.

The surface vortices can also be exploited to induce micro-mixing, as shown in figure 4 [9]. To quantify the mixing action, we conduct a pixel intensity analysis of the still grayscale image frames at various times. The time variation in the logarithmic standard deviation of the pixel intensities, normalised by the initial standard deviation, is plotted in figure 5(a) for a fixed applied frequency  $f$  but for different applied voltages  $V$ . Assuming a purely diffusive mechanism such that concentration homogenisation is anticipated to occur exponentially, the diffusivity  $D$ , which is a measure of the mixing intensity, can be estimated from a linear regression of figure 5(a) [7]. In other words, the slope of the curves in figure 5(a) is proportional to  $-D/L^2$ , where  $L$  is the characteristic length scale of the system, which we shall take to be the diameter of the microchamber, i.e.  $L \sim 10^{-3}$  m. The slope in figure 5(a) for the case when no electric field is applied, approximately  $-10^{-3}$ , gives a diffusivity  $D_o$  of  $10^{-9}$  m<sup>2</sup>/s, which is consistent with typical values for the diffusion coefficient. With applied electric fields, however, we observe the slope and hence the effective diffusivity  $D_{eff}$  to in-

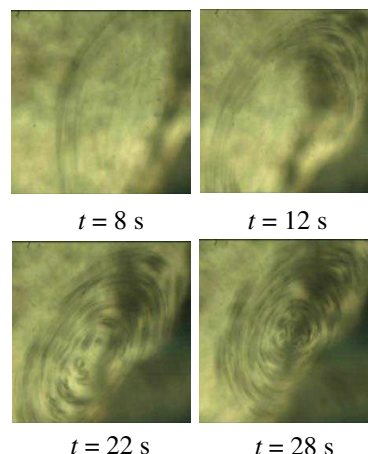


Figure 3: Rapid particle concentration in the surface vortices due to positive dielectrophoresis and shear-induced migration.

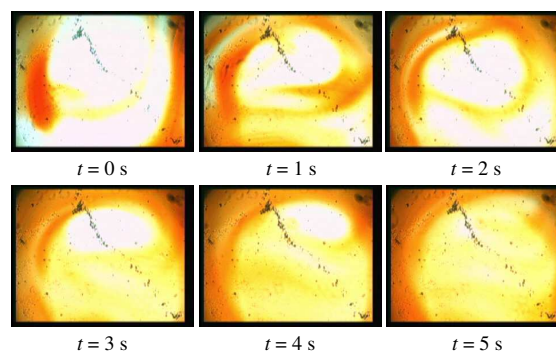


Figure 4: Rapid micro-mixing induced by surface vortex generation.

crease as the voltage is increased due to the effects of convective mixing induced by the liquid recirculation.

The ratio  $D_{eff}/D_o$  then reveals the extent of the intensification in the mixing relative to that in the absence of an applied electric field and hence flow. For the 70 kHz data plotted in figure 5(a), the mixing intensity is enhanced by up to two orders of magnitude at the highest applied voltage. This trend is also observed at other frequencies below 70 kHz. The effect of frequency is most clearly observed in figure 5(b), which is a plot of the logarithmic values of the applied field  $E \sim V/L$  and the ratio  $D_{eff}/D_o$ . The inset of figure 5(b) shows the slope of the  $\log E$  against  $\log(D_{eff}/D_o)$  data, indicating the exponent  $n$  with respect to  $E$  by which the mixing diffusivity scales as, i.e.  $(D_{eff}/D_o) \sim E^n$ . We acknowledge the poor reliability in the low frequency spectrum (10 kHz) of the data, especially at low voltages, since the ionic-wind driven liquid recirculation cannot be consistently generated as the applied voltages lie close to the critical boundaries for the existence of flow at this frequency (see figure 6). At high frequencies ( $\sim 70$  kHz), however, we observe the mixing diffusivity to scale almost quintically (to the 5<sup>th</sup> power) with respect to the field strength, much more intense than the quadratic field dependence obtained even for nonlinear electrokinetic devices [7]. It should be noted, however, that the two-dimensional pixel intensity analysis, independent of the chamber depth, can only give rise to approximate mixing diffusivities. Nevertheless, the secondary bulk recirculation which traverses the depth of the chamber, as shown in figure 2 is expected to further promote the mixing action.

The approach to the turbulent-like mixing intensities at high

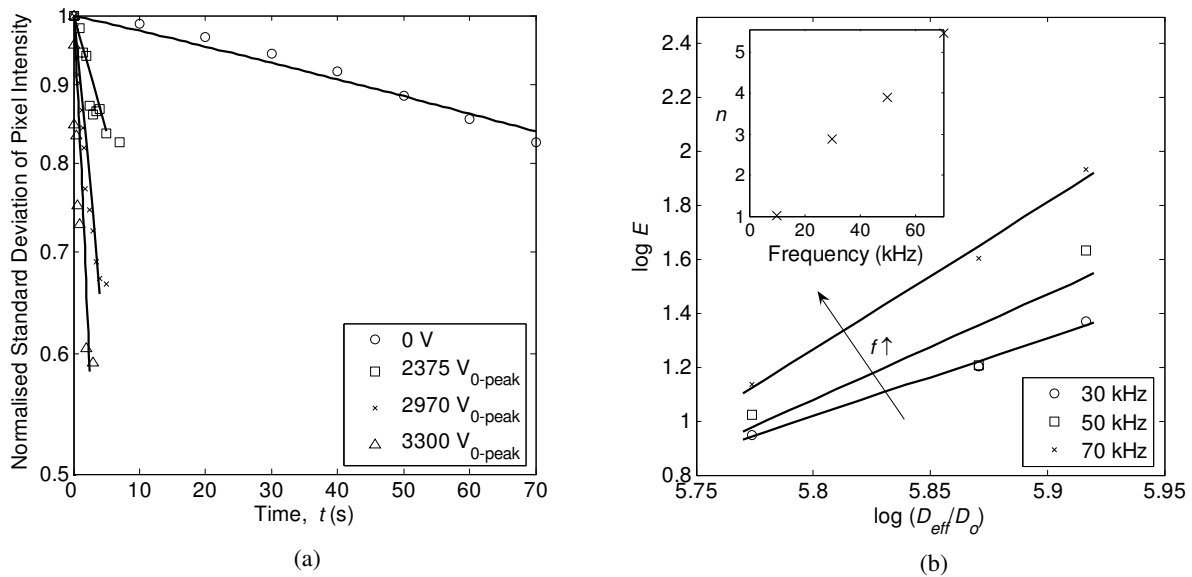


Figure 5: Convective enhancement of the mixing intensity through surface vortex flows. (a) Normalised standard deviation in the pixel intensity as a function of time for various applied voltages. The applied frequency is fixed at 70 kHz for the data shown. (b) Effect of the electric field  $E$  on the mixing intensity, as measured by the ratio between the effective diffusivity  $D_{eff}$  and the diffusivity in the absence of flow  $D_0$ , for various frequencies. The inset shows the variation in the exponent  $n$  representing the slope of the  $\log E$  against  $\log(D_{eff}/D_0)$  data with the applied frequency.

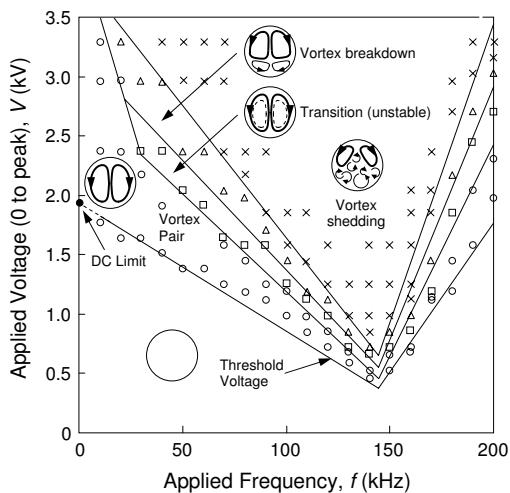


Figure 6: Delineation of the various flow recirculation patterns as a function of the applied voltage and applied frequency.

voltages and high frequencies is best explained by the mapping of the flow recirculation patterns in figure 6. As the voltage and frequency is increased, at least on the left half of the map below the optimum frequency of approximately 145 kHz, we observe the vortices to become unstable and eventually to breakdown, spawning off baby vortices. This vortex breakdown behaviour, reminiscent of that in Taylor-Couette flows, is most unique given the small Reynolds numbers encountered here. The successive breakdown in the vortices then gives rise to a cascade of vortices possessing a continuum of length scales, which, in turn, results in turbulent-like mixing [9]. More work is currently being undertaken to further quantify and elucidate the physical mechanism responsible for this chaotic behaviour, especially in the highly unstable region where vortex breakdown occurs. In any case, these very intense vortices provide a suitable mechanism to overcome the mixing deficiencies that typically plague microfluidic devices without the need for complex fabrication procedures associated with lamination micromixers.

### Secondary Bulk Recirculation

The bulk recirculatory flows can also be exploited for various microfluidic applications. In particular, we have shown the spiral tornado-like flow for the separation of red blood cells from blood serum [1, 8]. The red blood cells follow the liquid trajectory and hence are spun to a central stagnation point at the bottom of the chamber, as observed in figure 7. However, if the convective force is insufficient to overcome the sedimentation force, the red blood cells do not recirculate back up the central spinal column with the liquid. As such, a clear effluent of plasma is left above the thin Ekman boundary layer. The phenomenon is not unlike the paradox of tea leaves accumulating at the bottom of a stirred teacup, first elucidated by Einstein [3], which is a result of the Batchelor [2] flow arising between a fluid which is azimuthally rotated at the top surface and constrained at the bottom by a stationary plane. The technology then lends itself nicely as an essential step in the development of miniaturised point-of-care diagnostic kits.

### Conclusions

We present a new way of driving rapid liquid recirculation without the need for mechanically moving parts through interfacial shear by inducing a bulk electrohydrodynamic air flow above the liquid surface through the application of high frequency AC electric fields at a sharp electrode tip. The interfacial air drag results in both a primary surface liquid recirculation as well as a secondary bulk liquid motion, both of which have been demonstrated to be extremely useful for various microfluidic applications such as micro-mixing and particle separation/concentration/trapping. In particular, we show the surface vortices to be sufficiently intense, especially at high frequencies and voltages where the surface vortices iteratively break down to produce higher order generations of smaller vortices with successively smaller length scales, to drive turbulent-like micromixing. The surface vortices also act as an attractor for colloidal particles suspended in the liquid due to positive dielectrophoresis, thus constituting a useful mechanism by which particles can be concentrated or trapped. We also show that the secondary recirculation flow, which converges at a central

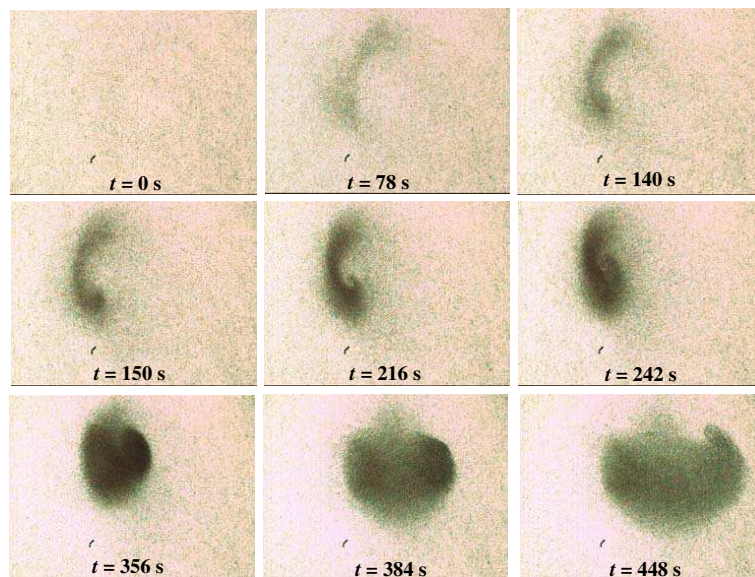


Figure 7: The secondary bulk recirculation in the form of a spiral-like flow is employed for rapid separation of red blood cells from blood plasma in the microfluidic chamber.

position at the bottom of the microfluidic chamber before re-circulating back up to the bulk via a central spinal column, is able to convect suspended particles in the bulk to a stagnation point at the bottom where the fluid converges. If the convection is insufficient to overcome the sedimentation of the particles at this stagnation point, particle trapping and concentration can be localised at this point.

The device therefore acts as a micromixer and a microcentrifuge, thus overcoming the difficulties of generating inertial/turbulence and centrifugal forces associated with many common microfluidic devices. Besides not requiring mechanical parts, the electrode is not in contact with the sample liquid, thus minimising Joule heating effects, generation of bubbles and ionic contaminants due to Faradaic reactions at the electrode, sample contamination and nonspecific adsorption of biological entities. Other advantages of the proposed devices are the inherent safety of high frequency AC fields despite the high voltages used, and the low current and hence low power requirement associated with the capacitive nature of the device enabling it to be driven by miniature portable battery packs.

## References

- [1] Arifin, D.R., Yeo, L.Y. and Friend, J.R., Microfluidic Blood Plasma Separation via Bulk Electrohydrodynamic Flows, *Biomicrofluidics*, **1**, 2007, 014103.
- [2] Batchelor, G.K., Note on the Class of Solutions of Navier-Stokes Equations Representing Steady Rotationally-Symmetric Flow, *Q. J. Mech. Appl. Math.*, **4**, 1951, 29–41.
- [3] Einstein, A., Die Ursache der Mäanderbildung der Flussläufe und des Sogenannten Baerschen Gesetzes. *Naturwiss.*, **14**, 1926, 223–224.
- [4] Leighton, D. and Acrivos, A., The Shear-Induced Migration of Particles in Concentrated Suspensions, *J. Fluid Mech.*, 1987, 415–439.
- [5] Pohl, H.A., *Dielectrophoresis*, Cambridge University Press, 1978.
- [6] Squires, T.M. and Quake, S.R., Microfluidics: Fluid Physics at the Nanoliter Scale, *Rev. Mod. Phys.*, **77**, 2005, 977–1026.
- [7] Wang, S.-C., Lai, Y.-W., Ben, Y. and Chang, H.-C. Microfluidic Mixing by dc and ac Nonlinear Electrokinetic Vortex Flows, *Ind. Eng. Chem. Res.*, **43**, 2004, 2902–2911.
- [8] Yeo, L.Y., Friend, J.R. and Arifin, D.R., Electric Tempest in a Teacup: The Tea Leaf Analogy to Microfluidic Blood Plasma Separation, *Appl. Phys. Lett.*, **89**, 2006, 103516.
- [9] Yeo, L.Y., Hou, D., Maheshwari, S. and Chang, H.-C., Electrohydrodynamic Surface Microvortices for Mixing and Particle Trapping, *Appl. Phys. Lett.*, **88**, 2006, 233512.